imperfect radiosonde observations. Model physics becomes important when the model extrapolates to locations and times far from the ground truth provided by radiosondes. However, radiosonde temperatures are themselves imperfect and require corrections for absorption of solar and infrared radiation, thermal emission, and conduction and convection of heat (*21*). Inadequate calibration could contribute to the temperature biases seen in Fig. 4B, to the extent that the model is constrained by radiosondes in this region.

Figures 2 through 5 indicate that future measurements, if available in near real-time, could play a significant role in numerical weather prediction (NWP). The density of 500 globally distributed measurements per day provided by a single orbiting GPS receiver would exceed that of the radiosonde network by a factor of 2 in the Southern Hemisphere, making a significant contribution to the global observing system. A constellation of orbiting receivers could make a major contribution to fulfilling the stated temperature observation requirements for global NWP. The results presented here demonstrate desirable properties for use in NWP, namely generally good agreement with a high-quality NWP analysis, plus the ability to identify a minority of cases where there is room for significant improvement in the analysis.

REFERENCES AND NOTES

1. G. F. Fjeldbo, V. R. Eshleman, A. J. Kliore, *Astron. J.* **76**, 123 (1971).
2. G. F. Lindal, *J. Geophys. Res.* **84**, 8443 (1979); A. J. Kliore and I. R. Patel, *ibid.* **85**, 7957 (1980).
3. D. P. Hinson and J. A. Magalhaes, *Icarus* **94**, 64 (1991).
4. G. F. Lindal, *Astron. J.* **103**, 967 (1992).
5. Atmospheric radio occultation observations using a GPS receiver in low Earth orbit were proposed and developed for the National Aeronautics and Space Administration's (NASA's) Earth Observing System in 1988 (*22*), but the concept became a reality with the launch of the University Corporation for Atmospheric Research (UCAR) GPS-MET experiment on 3 April 1995 (*23*).
6. A. C. Lorenc, *Mon. Weather Rev.* **109**, 701 (1981); D. B. Shaw, P. Lonnberg, A. Hollingsworth, P. Unden, *Q. J. R. Meteorol. Soc.* **113**, 533 (1987).
7. E. R. Kursinski, G. A. Hajj, K. R. Hardy, in *Proceedings of the 8th Symposium on Meteorological Observations and Instrumentation*, Anaheim, CA, 17 to 22 January 1993 (American Meteorological Society, Boston, MA, 1993), pp. J153–J158.
8. ———, *Proceedings of the SPIE Symposium on Optical Engineering and Photonics in Aerospace Science and Sensing, Paper 1935-13* (1993).
9. K. R. Hardy, G. A. Hajj, E. R. Kursinski, *Int. J. Satell. Commun.* **12**, 463 (1994).
10. G. D. Thayer, *Radio Sci.* **9**, 80 (1974).
11. To obtain the accuracies necessary for atmospheric work, we used a modified version of the GIPSY–OASIS II system developed at the Jet Propulsion Laboratory for the Ocean Topography Experiment (TOPEX/Poseidon) to determine receiver and transmitter orbits, and to calibrate and remove receiver and transmitter clock biases and instabilities (*9, 24*). Vertical smoothing, decreasing from ~1.4 km in the stratosphere to ~0.5 km near the surface, was also applied to the Doppler frequency measurements to make them consistent with the Fresnel diffraction resolution limit (*3, 7*). Finally, unwanted dispersive ionospheric contributions to bending were removed by forming a linear combination of the bending angles estimated independently for each of the two GPS signal frequencies (*25*).
12. G. A. Hajj, E. R. Kursinski, W. I. Bertiger, L. J. Romans, K. R. Hardy, in *Proceedings of the 7th Conference on Satellite Meteorology and Oceanography*, Monterey, CA, 6 to 10 June 1994 (American Meteorological Society, Boston, MA, 1994), pp. J7–J10.
13. E. R. Kursinski, G. A. Hajj, K. R. Hardy, L. J. Romans, J. T. Schofield, *Geophys. Res. Lett.* **22**, 2365 (1995).
14. D. P. Hinson and G. L. Tyler, *Icarus* **54**, 337 (1983); D. P. Hinson and J. A. Magalhaes, *ibid.* **105**, 142 (1993); D. P. Hinson and J. M. Jenkins, *ibid.* **114**, 310 (1995).
15. D. G. Andrews, J. R. Holton, C. B. Leovy, *Middle Atmosphere Dynamics* (Academic Press, Orlando, FL, 1987).
16. E. R. Kursinski, G. A. Hajj, K. R. Hardy, *Eos* **72**, 372 (1991); M. Bevis *et al.*, *J. Geophys. Res.* **97**, 15787 (1992); L. L. Yuan *et al.*, *ibid.* **98**, 14925 (1993).
17. D. O'C. Starr and S. H. Melfi, *NASA Conf. Publ. 3120* (May 1991).
18. W. L. Smith, H. M. Woolf, C. M. Hayden, D. Q. Wark, L. M. McMillan, *Bull. Am. Meteorol. Soc.* **60**, 1177 (1979).
19. J. R. Eyre, G. A. Kelly, A. P. McNally, E. Andersson, A. Persson, *Q. J. R. Meteorol. Soc.* **119**, 1427 (1993).
20. B. J. Hoskins, M. E. McIntyre, A. W. Robertson, *ibid.* **111**, 877 (1985).
21. J. K. Luers and R. E. Eskridge, *J. Appl. Meteorol.* **34**, 1241 (1995).
22. T. P. Yunck, G. F. Lindal, C. H. Liu, *Proceedings of IEEE Positioning, Location, and Navigation Symposium*, Orlando, FL, 29 November to 2 December 1988, pp. 251–258.
23. R. Ware *et al.*, *Bull. Am. Meteorol. Soc.* in preparation.
24. W. I. Bertiger *et al.*, *J. Geophys. Res.* **99**, 24449 (1994).
25. V. V. Vorob'ev and T. G. Krasil'nikova, *Izv. Akad. Nauk SSSR Fiz. Atmos. Okeana* **29**, 626 (1993).

26. The research described here was largely performed at the Jet Propulsion Laboratory, California Institute of Technology, supported jointly by NASA and the California Institute of Technology through the Caltech President's fund. We are grateful to our collaborators, GPS-MET principal investigator R. Ware and project manager M. Exner, of the UCAR, Boulder, CO, for providing us with access to raw flight data from the GPS-MET experiment. We also thank the ECMWF for providing us with atmospheric data, software, and assistance with data interpretation and M. E. Gelman of the National Meteorological Center (NMC) for many useful discussions on the NMC radiosonde data set.

11 September 1995; accepted 28 December 1995

Observations of Carbon Monoxide in Comet Hale-Bopp

David Jewitt,* Matthew Senay,* Henry Matthews

The recently discovered comet Hale-Bopp (C/1995 O1) sports a bright dust coma even though it is still far from the sun (presently 6 astronomical units). This feature has attracted considerable interest in the public and scientific arenas. The comet is headed toward perihelion at 0.92 astronomical unit in April 1997 and is widely expected to then become a spectacular naked-eye comet. With millimeter-wave observations, carbon monoxide (CO) has been identified as the driver for the early activity observed in Hale-Bopp.

Activity in comets near the sun is known to be driven by the sublimation of water ice from the nucleus in response to strong solar heating (*1*). Comet Hale-Bopp belongs to a class of comets that are too distant and too cold for water ice to sublimate, raising the possibility that the activity creating its dust coma is driven by the sublimation of a more volatile ice or even by another physical process. Historically, activity in distant comets has been attributed to heat released by exothermic phase changes in water ice, explosive reactions between radicals in the nucleus, collisions with interplanetary boulders, or the outgassing of embedded supervolatiles such as carbon monoxide, carbon dioxide, and nitrogen. The advent of sensitive millimeter-wave telescopes allows us to search directly for outgassed supervolatiles.

We first observed Hale-Bopp in September 1995 using the 15-m-diameter James Clerk Maxwell Telescope (JCMT) atop Mauna Kea, Hawaii. We studied the J = 2-1 rotational transition of CO at 230 GHz. At the time of observation, Hale-Bopp was at a heliocentric distance of 6.6 astronomical units (AU). Nearby position and flux standards were also observed, from which we estimated a pointing accuracy of ±2 arc sec. The diameter of the circular JCMT beam subtended 20 arc sec on the sky (corresponding to 9.3×10^7 m at the comet), which is large compared with the pointing uncertainties.

The comet appeared projected against the center of our galaxy (Fig. 1), producing a nonuniform background of diffuse emission from interstellar CO along the line of sight. Cometary CO emission was detected on 5 and 7 September 1995 [universal time (UT)] but appeared partially confused with background CO lines and noise because of

D. Jewitt and M. Senay, Institute for Astronomy, Honolulu, HI 96822, USA.
H. Matthews, Joint Astronomy Centre, Hilo, HI 96720, USA, and Herzberg Institute of Astrophysics, Ottawa, ON K1A 0R6, Canada.

*Visiting Astronomer at the James Clerk Maxwell Telescope, operated by the Royal Observatory, Edinburgh, on behalf of the Particle Physics and Astronomy Research Council of the United Kingdom, the Netherlands Organization for Scientific Research, and the National Research Council of Canada.

Table 1. Parameters of the Hale-Bopp CO[2-1] line. The date given is the midpoint of integration. Abbreviations: R, heliocentric distance; D, geocentric distance; a, phase angle in degrees; t, integration time; v_g, geocentric radial velocity of Hale-Bopp; v_o, observed line velocity; $dv = v_o - v_g$; T_A, peak antenna temperature; $T_A dv$, line area; Q_{CO}, CO production rate (molecules per second).

Date (1995 UT)	R (AU)	D (AU)	a (deg)	t (s)	v_g (km s^{-1})	v_o (km s^{-1})	dv (km s^{-1})	T_A (K)	$T_A dv$ (K km s^{-1})	Q_{CO} (10^{28} s^{-1})
Sep. 5, 7*	6.760	6.335	8.01	10,800	12.62	12.30 ± 0.04	−0.32 ± 0.02	0.06	0.029 ± 0.006	1.8
Sep. 19.22	6.649	6.437	8.61	11,400	14.31	13.98 ± 0.04	−0.33 ± 0.04	0.08	0.042 ± 0.008	2.5
Sep. 20.21	6.640	6.445	8.64	11,400	14.38	13.96 ± 0.02	−0.42 ± 0.02	0.11	0.031 ± 0.006	1.8
Oct. 16.12	6.414	6.657	8.48	4,800	12.98	12.62 ± 0.02	−0.36 ± 0.02	0.26	0.057 ± 0.010	3.0
Oct. 30.15	6.290	6.751	7.74	6,000	9.93	9.71 ± 0.06	−0.22 ± 0.06	0.10	0.067 ± 0.013	4.1
Nov. 13.09	6.165	6.816	6.60	7,200	5.73	5.43 ± 0.10	−0.30 ± 0.10	0.10	0.073 ± 0.014	4.7

*Average of spectra taken on two nights.

high air-mass and system temperature. Firm detections, devoid of significant background contamination, were first obtained on 19 and 20 September (*2*) (Fig. 2). Subsequently, observations of the line were reported from the IRAM (Institute de Radio Astronomie Millimetrique) 30-m telescope (*3*). The core of the line is unresolved (at spectral resolution ~0.2 km s^{-1}) and appears systematically blueshifted with respect to the geocentric radial velocity of the comet by about 0.35 km s^{-1}. We take this as a measure of the coma outflow speed. Day-to-day differences in the blueshift (Table 1) are significant and may reflect variations in the direction of outgassing, perhaps associated with rotation of the nucleus. In addition, there is a faint redshifted wing to the line, which suggests weak emission from the night side of the nucleus.

The integrated intensity of the CO line increased linearly from 5 September to 13 November (Fig. 3), showing that the outgassing rate increased by a factor of 2 in just 2 months. The time taken for a molecule to travel from the center to the edge of the JCMT beam at 0.35 km s^{-1} is $t_c \approx 10^5$ s (about 1 day), and variability on similar or shorter time scales cannot be observed (*4*). The CO brightening is so dramatic (the dependence on heliocentric distance is about $R^{-9.4}$) that it cannot plausibly be sustained until perihelion (the extrapolated outgassing would then be 10^{11} kg s^{-1}). Presumably we are witnessing a transient brightening akin to those seen already in CO from periodic comet Schwassmann Wachmann 1 (SW1) (*5*, *6*) and optically in 2060 Chiron (*7*). This scenario would be consistent with reported smaller line areas of <0.049 K km s^{-1} (3σ) on 8 December and 0.028 ± 0.004 K km s^{-1} on 9 December (*8*).

We assume that CO is a parent molecule and not the decay product of a more complex molecule. Of the possible parents, CO_2 photodissociates to CO too slowly at 6.6 AU [the time constant is $t_{photo} \sim 10^8$ s (*9*)] to constitute a viable source. The photodissociation of formaldehyde (H_2CO) is more rapid ($t_{photo} \sim 3 \times 10^6$ s), but this molecule is undetected down to 1.5% of the CO production (*10*).

At 6.6 AU, the photodestruction time for CO is $t_i \approx 6 \times 10^7$ s (*9*). This exceeds t_c by nearly two orders of magnitude, so that photodestruction may be neglected in the calculation of the production rate. The time scale to reach fluorescence equilibrium at 6.6 AU is $t_f \approx 10^6$ s (*11*). With $t_f > t_c$, the population of the rotational levels in CO in the JCMT beam must be determined largely by intermolecular collisions. To estimate the production rate Q, we assumed a Boltzmann distribution of rotational energies with a rotational temperature of 10 K, this being the measured value in SW1 (*6*). The average is $Q_{CO} = 2.8 \times 10^{28}$ s^{-1} (1300 kg s^{-1}) (Table 1). For comparison, a water mass loss rate of 10^3 kg s^{-1} was attained by comet Halley only when near preperihelion, at about 2 AU (*12*).

Does the strong outgassing from Hale-Bopp suggest that its nucleus is unusually large? Consideration of the rate of sublimation of CO does not support such a conclusion. We calculated the flux of molecules sublimated from CO and H_2O ice surfaces (Fig. 4). The calculations assume sublimation in thermal equilibrium but neglect thermal conduction. Two curves for each volatile show the dependence of the sublimation rate on the (unknown) nuclear spin. At 6.6 AU, the CO sublimation fluxes vary between 5×10^{20} m^{-2} s^{-1} (isothermal nucleus) and 2×10^{21} m^{-2} s^{-1} (subsolar patch). The nominal $Q_{CO} = 2.8 \times 10^{28}$ s^{-1} could be sustained by an exposed patch of CO having an area $A = 14$ to 56 km^2, corresponding to a circle of radius $(A/\pi)^{1/2} = 2.1$ to 4.2 km. This constitutes a lower limit to the radius of the nucleus.

Outgassing from near-sun comets is largely confined to small, active vents embedded in a crust or mantle of nonvolatile material (*4*, *13*). Two characteristics of Hale-Bopp are most naturally explained in terms of outgassing from localized vents on the nucleus. First, the systematic blueshift of the line peak (Table 1 and Fig. 2) indicates sunward ejection in a collimated jet. The dominance of the sunward (day-side) emission further shows that the sublimation rate is sensitive to the diurnal temperature variation and hence is produced close to the surface (presumably within one thermal skin depth, or about 10 cm for a rotational period of 10 hours). The velocity of ejection (0.35 km s^{-1}) is higher than that expected for adiabatic expansion of CO (0.2 km s^{-1}). The velocity excess may result from heating by flow through a porous surface layer (*6*) or, more likely, by dust heating (*14*). Second, the optical image shows a collimated (dust) jet such as would be produced by gas flow into vacuum from an active vent. We surmise that Hale-Bopp resembles better studied comets, in that it outgasses from the near-surface regions in one or more active vents that together occupy only a small fraction of the nuclear surface. Hale-Bopp's previous orbit had perihelion distance $0.5 \leq q \leq 1.5$ AU (*15*), providing ample opportunity for the formation of a rubble mantle by capture of suborbital debris on the nucleus.

In comet Halley, the unmantled fraction of the surface was ~10% (*13*). With this active fraction, the nucleus radius of Hale-Bopp would be 3 to 7 km, which is similar to the 5-km effective radius of Halley and other short-period comets (*4*). In any event, sustained outgassing of CO accounts naturally for the extended coma and elevated brightness of Hale-Bopp, without assuming that the nucleus is unusually large. Even the reported detection of this comet at magnitude 18 at 13.1 AU on 27 April 1993 (*16*) is compatible with coma production by CO. The sublimation rate at 13.1 AU would be reduced relative to that at 6.6 AU by a factor $(6.6/13.1)^2 \sim 0.25$ (Fig. 4), or $Q_{CO} \sim 300$ kg s^{-1}. In the period of observations covered, Hale-Bopp lost ~10^{35} molecules of CO, or total mass 6×10^9 kg. This corresponds to a very modest thickness of 0.6 m of CO ice (of density 1000 kg m^{-3}) spread over a 10-km^2 vent.

In situ observations of CO in comet Halley showed a distributed near-nucleus source in addition to a nuclear component (*17*). The asymmetric CO line in Hale-Bopp is incompatible with a spherically distributed near-nucleus source inferred around Halley (*17*), although we cannot eliminate the possibility that a fraction of the observed CO molecules emanate from grains in the near-nucleus coma (*18*).

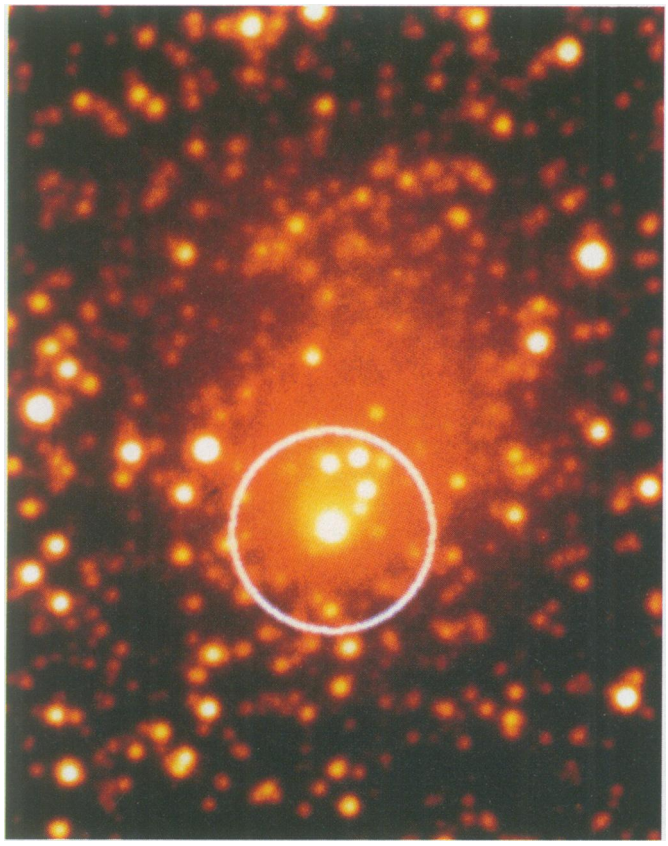

Fig. 1. Charge-coupled device image of comet Hale-Bopp taken on 20 September 1995 (UT) at the University of Hawaii 2.2-m telescope. The white circle is centered on the optocenter and denotes the 20-arc sec (9.3×10^7 m) diameter JCMT beam. The image, which was taken simultaneously with JCMT data, shows the asymmetric distribution of dust in the coma. North is to the top, east to the left.

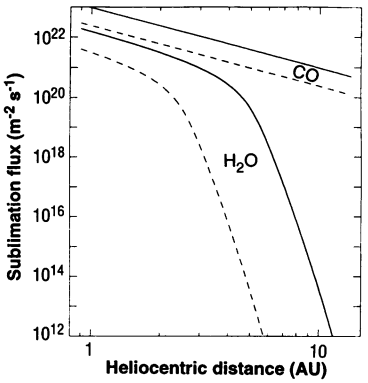

Fig. 4. Sublimation of water and CO ices as a function of heliocentric distance. The sublimation flux was calculated for two cases for each distance, assuming sublimation in thermal equilibrium with sunlight: a vertically illuminated volatile surface (solid lines) and an isothermal nucleus (dashed lines). The two cases bracket the maximum and minimum temperatures and sublimation rates for each volatile under different states of the nucleus rotation (*24*).

Water ice was reported in the coma of Hale-Bopp (*19*). Presumably, water ice grains are expelled from the nucleus by the more volatile CO. They remain solid because of the low insolation at 6.6 AU (the blackbody temperature at this distance is only 108 K). The sublimation lifetime of a spherical grain of water ice of density 1000 kg m^{-3} and radius a (in micrometers) is $t_{sub} = 10^{22}(a/Z)$ (in seconds), where Z is the sublimation flux (per square meter per second). The neutral optical–near infrared colors of the coma (*20*) suggest $a \geq 2$ μm. For isothermal blackbody grains at 6.6 AU, $Z = 10^{11}$ m^{-2} s^{-1} (Fig. 4), and a 2-μm grain has $t_{sub} \sim 2.2 \times 10^{11}$ s = 7000 years (the temperature of real grains might be slightly higher and the lifetime slightly lower owing to wavelength-dependent emissivity effects). Sublimation of the water ice component will first change the morphology of the coma when t_{sub} is comparable to the residence time in the JCMT beam, t_c. With $t_c = t_{sub} \sim 1$ day, we obtain $Z = 2 \times 10^{17}$ m^{-2} s^{-1}, which will occur at $R = 3.5$ AU (Fig. 4). Therefore, we anticipate the disappearance of the water ice grains from the coma of Hale-Bopp near 3 AU, after which the bulk of the water will instead be emitted directly from the nucleus. Gaseous OH production may show a local maximum near this time, as the coma ice grains sublimate. A similar preperihelion OH surge was observed near 4.5 AU in the distant comet Bowell (1982 I) (*21*).

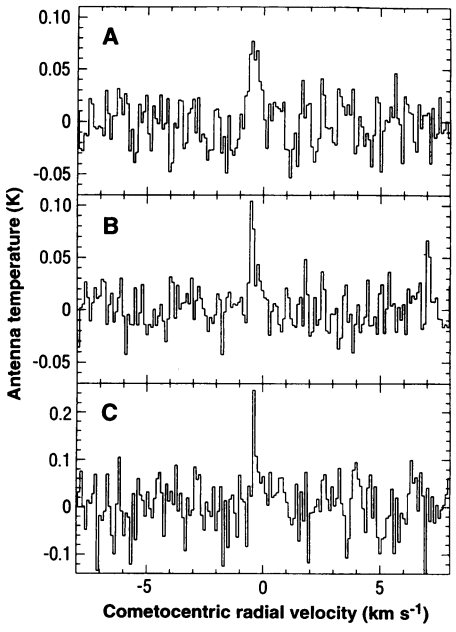

Fig. 2. CO 2-1 rotational emission from Hale-Bopp. Sample observations from (**A**) 19 September, (**B**) 20 September, and (**C**) 16 October 1995 (UT) are shown.

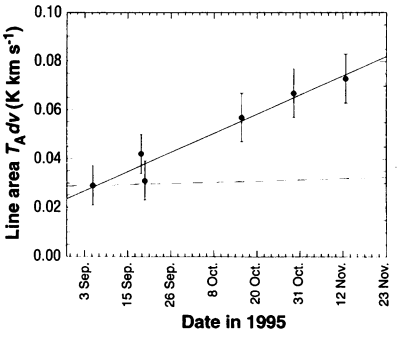

Fig. 3. Measured area of the CO[2-1] line versus the date of observation. Error bars denote formal uncertainties from a line-plus-Gaussian fit to the data. The dashed line shows the variation expected if Q_{CO} maintains thermal equilibrium sublimation (that is, $Q_{CO} \propto R^{-2}$). The solid line shows $Q_{CO} \propto R^{-9.4}$.

The peak perihelion brightness of Hale-Bopp cannot be meaningfully predicted from the available data. Given an unlimited surface supply, the CO production rate should increase as R^{-2}, with a concomitant increase in the ejected dust and a brightness at visual wavelengths increasing roughly as R^{-4}. A much faster rise is apparent in Fig. 3. However, it is quite possible that the near-surface CO reservoir is limited and that the CO production rate will actually decrease as the comet approaches the sun. This would be the case, for example, if only a limited amount of CO migrated to the near-surface regions in response to internal conduction during the previous orbit (*22*). Water ice sublimation will become strong near 3 to 4 AU (summer 1996), but the magnitude of the water production rate ultimately depends on the (unknown) area of the exposed water ice vents and their orientation to the sun. If the water vents occupy an effective subsolar area similar to the 14 km^2 of CO, the perihelion water production should amount to $Q_{H_2O} \approx 2.8 \times 10^{29}$ s^{-1} (8400 kg s^{-1}), and Hale-Bopp will rival, but not surpass, Halley in mass loss. However, in view of the obvious differences with Halley al-

ready apparent at 6 AU, this estimate must be considered as highly uncertain.

In many respects, Hale-Bopp resembles SW1. Both display activity when far from the sun (*23*), both show optical dust jets indicating anisotropic mass loss from the nucleus, and both are prodigious sources of CO [2000 kg s^{-1} for SW1 (*5*, *6*)]. However, whereas SW1 has a nearly circular trans-Jovian orbit that prevents a close approach to the sun, the orbit of Hale-Bopp is highly eccentric, and the solar insolation at the nucleus will increase by a factor of 50 between now and perihelion. Thus, Hale-Bopp provides an unprecedented opportunity to study the development of CO and H_2O outgassing in a comet that is still far from perihelion.

REFERENCES AND NOTES

1. F. Whipple, *Astrophys. J.* **111**, 375 (1950).
2. H. Matthews, D. Jewitt, M. Senay, *Int. Astron. Union Circ. 6234* (21 September 1995).
3. H. Rauer *et al.*, *Int. Astron. Union Circ. 6236* (25 September 1995).
4. D. C. Jewitt, in *Comets In The Post-Halley Era*, R. Newburn, M. Neugebauer, J. Rahe, Eds. (Kluwer, Dordrecht, 1991), pp. 19–65.
5. M. Senay and D. Jewitt, *Nature* **371**, 229 (1994).
6. J. Crovisier *et al.*, *Icarus* **115**, 213 (1995).
7. J. Luu and D. Jewitt, *Astron. J.* **100**, 913 (1990).
8. M. Womack, S. A. Stern, M. Festou, *Int. Astron. Union Circ. 6276* (21 December 1995).
9. W. F. Huebner, J. J. Keady, S. P. Lyon, *Solar Photo Rates for Planetary Atmospheres and Atmospheric Pollutants* (Kluwer, Dordrecht, 1992), p. 273.
10. J. Crovisier *et al.*, abstract at 27th Annual Meeting of the American Astronomical Society Division for Planetary Sciences, Kona, Hawaii, 9 to 13 October 1995.
11. J. Crovisier and J. Le Bourlot, *Astron. Astrophys.* **123**, 61 (1983).
12. F. P. Schloerb, M. J. Claussen, L. Tacconi-Garman, *ibid.* **187**, 469 (1987).
13. H. U. Keller *et al.*, *ibid.*, p. 807.
14. D. C. Boice, W. F. Huebner, S. A. Stern, in *Workshop on the Activity of Distant Comets*, W. Huebner *et al.*, Eds. (Southwest Research Institute Press, San Antonio, TX, 1993), pp. 134–139.
15. M. Bailey *et al.*, in preparation.
16. R. H. McNaught, *Int. Astron. Union Circ. 6198* (2 August 1995).
17. P. Eberhardt *et al.*, *Astron. Astrophys.* **187**, 481 (1987).
18. N. H. Samarasinha and M. Belton, *Icarus* **108**, 103 (1994).
19. J. Davies, T. Geballe, D. Cruikshank, T. Owen, C. de Bergh, *Int. Astron. Union Circ. 6225* (11 September 1995).
20. M. Hicks, *Int. Astron. Union Circ. 6200* (3 August 1995).
21. M. A'Hearn, D. G. Schleicher, P. D. Feldman , R. L. Millis, D. T. Thompson, *Astron. J.* **89**, 579 (1984).
22. D. Prialnik, *Adv. Space Res.* **9**, 25 (1989).
23. D. C. Jewitt, *Astrophys. J.* **351**, 277 (1990).
24. Thermodynamic parameters of the ices were taken from G. N. Brown and W. T. Ziegler, *Adv. Cryog. Eng.* **25**, 662 (1979). The Bond albedo and emissivity were taken to be 0.04 and 1.0, respectively. Thermal conduction was neglected: its effects would decrease the sublimation fluxes relative to the values plotted here. Neither the rotation state of the Hale-Bopp nucleus nor the conductivity of its surface materials are known.

25. We thank the JCMT operators for help observing, K. Chambers for the image in Fig. 1, and D. Tholen for providing perturbed ephemerides. D.J. appreciates support from the National Aeronautics and Space Administration's Origins of Solar Systems Program.

26 December 1995; accepted 1 February 1996

Imitation of *Escherichia coli* Aspartate Receptor Signaling in Engineered Dimers of the Cytoplasmic Domain

Andrea G. Cochran* and Peter S. Kim

Transmembrane signaling by bacterial chemotaxis receptors appears to require a conformational change within a receptor dimer. Dimers were engineered of the cytoplasmic domain of the *Escherichia coli* aspartate receptor that stimulated the kinase CheA in vitro. The folding free energy of the leucine-zipper dimerization domain was harnessed to twist the dimer interface of the receptor, which markedly affected the extent of CheA activation. Response to this twist was attenuated by modification of receptor regulatory sites, in the same manner as adaptation resets sensitivity to ligand in vivo. These results suggest that the normal allosteric activation of the chemotaxis receptor has been mimicked in a system that lacks both ligand-binding and transmembrane domains. The most stimulatory receptor dimer formed a species of tetrameric size.

Bacterial chemotaxis, the regulated swimming behavior of bacteria in an attractant or repellent gradient, is one of the most thoroughly studied and biochemically defined signaling processes (*1*, *2*). Determination of the structures of the dimeric ligand-binding domain of the *Salmonella typhimurium* aspartate receptor in apo and aspartate-bound forms was an important step toward understanding the transmembrane signaling mechanism (*3*). However, it is not obvious from these structures how periplasmic ligand binding triggers events in the cytoplasm. Aspartate binding induces only a small rotation of ~4° between monomers (about an axis parallel to the membrane and perpendicular to the twofold symmetry axis). Consistent with this structural view, disulfide cross-linking and nuclear magnetic resonance studies suggest that ligand binding results in small shifts in the relative positions of the transmembrane helices (*4*, *5*). Several types of interhelical motion have been suggested as possible signaling mechanisms: Examples include pistonlike movements, scissoring motions, and supercoiling of helices (*4*). Presumably, these adjustments in helix orientation reach the cytoplasmic portion of the receptor and are transmitted through the adapter protein CheW to the kinase CheA, thereby inhibiting phosphorylation of the diffusible messenger CheY (Fig. 1).

To extend structural and mechanistic studies to the cytoplasmic receptor-kinase complex, we engineered dimers of the *E. coli* aspartate receptor (Tar) cytoplasmic domain in which the monomers are held in parallel, as in the intact receptor (Fig. 1). The desired orientation was achieved by fusing the receptor domain to the short, parallel coiled-coil dimerization domain (leucine zipper) from the transcriptional activator GCN4 (*6*, *7*). In addition to providing a dimerization domain, the GCN4 peptide replaces the receptor sequence that presumably relays transmembrane conformational changes to the cytoplasm (*8*). Fusion to a stable, inflexible structural element fixes the structure of the receptor fragment in this critical region.

No detailed structural information is available to guide the design of a dimer of the Tar cytoplasmic domain. However, clues can be found in two cytoplasmic regions of the receptor that are associated with the process of adaptation (*1*, *2*).

Efficient gradient sensing requires continuous adjustment of receptor sensitivity. Attractant stimulation induces a net increase in methylation of four specific glutamic acid side chains (Fig. 2A), catalyzed by the methyl transferase CheR. Methylation of these glutamic acids, or mutation to glutamine, desensitizes the receptor to attractant ligands (*9*–*11*). Conversely, loss of attractant stimulation results in net demethylation by the methyl esterase CheB. The kinase activity of receptor-associated CheA, in the absence of ligand, increases in direct response to increases in receptor methylation or amidation (*11*–*13*), suggesting that structural changes related to receptor adaptation are intimately linked to the conformational changes that occur during receptor signaling.

The primary sequences of both methylation regions (K1 and R1; Fig. 2A) conform to seven-residue repeating patterns (4-3 hydrophobic repeats) typical of α-helical coiled coils (*2*, *14*). The seven-residue spacing of the three K1 methylation sites would align them on one face of a coiled-coil helix (*2*). Receptor point mutations that transform cells to an extreme smooth-swimming phe-

Howard Hughes Medical Institute, Whitehead Institute for Biomedical Research, Department of Biology, Massachusetts Institute of Technology, Nine Cambridge Center, Cambridge, MA 02142, USA.

*To whom correspondence should be addressed.